

Magnetic excitations in the sinusoidal spin phase of Er and Tm

S. H. Liu

Department of Physics, University of California, San Diego, La Jolla, California 92093-0319

J. F. Cooke

Solid State Division, Oak Ridge National Laboratory, Oak Ridge, Tennessee 37830-6032

(Received 22 January 1996)

The frequency moment method is used to study the magnetic excitations in magnetically ordered systems, especially the sinusoidally modulated spin structure that occurs just below the Néel temperatures of erbium and thulium. It is shown that the transverse excitations may have rather sharp but dispersionless spectra or broad spectra depending on the relative strengths of the twofold anisotropy energy versus the exchange energy. The longitudinal spin excitations are extensions of the Goldstone modes. They may have rather sharp spectra with linear dispersion relations when the exchange and anisotropy energies are comparable. [S0163-1829(96)03222-5]

I. INTRODUCTION

The rare-earth metals erbium (Er) and thulium (Tm) have the sinusoidally modulated spin structure in a range of temperature immediately below their magnetic ordering temperatures.^{1,2} The spins in each hexagonal plane of the crystal are ferromagnetically aligned in the direction perpendicular to the plane, and the size of the ordered moment varies sinusoidally from plane to plane with a periodicity that is usually not an integral multiple of the crystal c -axis repeat distance. This is a special case of a class of periodic spin structures which can be characterized by a wave vector \mathbf{Q} , which points along the c -axis direction. Nishikubo and Nagamiya³ showed that this kind of spin ordering arises due to an interplay of the long-range exchange interaction, which favors a periodic spin arrangement, and a uniaxial anisotropy, which forces the spins to lie in the c direction. Cooper⁴ discussed the equations of motion of the spin in the sinusoidally modulated phase and pointed out that the elementary excitations are not ordinary spin waves. One of the present authors (S.H.L.) put the solution of the spin-excitation problem in the form of an infinite continued fraction,⁵ and argued that the excitation spectrum is inherently broad, due to the spatial fluctuations of the local exchange and anisotropy fields. Neutron-scattering studies carried out by Wakabayashi and Nicklow⁶ have detected broad inelastic responses around the magnetic satellites, in qualitative agreement with theoretical conclusions. The authors also reported rather sharp lines for longitudinal excitations which have linear dispersion relations. There has been no explanation for these modes so far.

In this paper we reexamine the magnetic excitation problem by using a new method, the method of frequency moments. The excitation is defined as the linear response of the spin system to an external excitation, e.g., inelastic scattering of neutrons. For a fixed wave vector of the excitation, the frequency spectrum is determined indirectly by calculating the moments of the frequency, or energy, of the excitation. In principle, it requires an infinite number of moments to define the spectrum uniquely. In practice, however, only a few low-

order moments are needed to find a spectral shape which can be compared with experiments. The paper is organized as follows. Section II formulates the frequency moment method for the spin system, and demonstrates its use by reproducing the known results for the isotropic Heisenberg ferromagnet. Section III reviews the stability criterion for the sinusoidal spin structure. Section IV applies the frequency moment method to the transverse spin excitations. Section V does the same for longitudinal spin excitations. The theoretical results are compared with experiments in Sec. VI.

II. THE FREQUENCY MOMENT METHOD

The frequency moment method is a well-established scheme to calculate the phonon density of states for an elastic solid.⁷ To the extent the authors are aware, it has not been applied to magnetic systems, certainly not to the sinusoidally modulated spin systems. It is, therefore, helpful to outline the method briefly and illustrate its use by reproducing some well-known results for the isotropic Heisenberg ferromagnet.

The Hamiltonian of the ferromagnetic system is

$$H_0 = -J \sum_{i,\delta} \mathbf{S}_i \cdot \mathbf{S}_{i+\delta}, \quad (1)$$

where the sum on i is over all lattice sites and σ is over all nearest neighbors of i . The ordered moment points in the z direction. The operator for a spin excitation with wave vector \mathbf{q} are $S_{\mathbf{q}}^{\pm}$ defined by

$$S_{\mathbf{q}}^{\pm} = N^{-1/2} \sum_i (S_i^x \pm iS_i^y) e^{i\mathbf{q} \cdot \mathbf{r}_i}, \quad (2)$$

where N is the number of lattice sites, and \mathbf{r}_i is the coordinate vector of the i th site. The propagator of the excitation is

$$G(\mathbf{q}, t) = \langle T S_{\mathbf{q}}^+(t) S_{-\mathbf{q}}^-(0) \rangle, \quad (3)$$

where the Heisenberg operator is, in units with $\hbar=1$,

$$S_{\mathbf{q}}^+(t) = e^{iH_0 t} S_{\mathbf{q}}^+ e^{-iH_0 t}. \quad (4)$$

The frequency spectrum $G(\mathbf{q}, \omega)$ is the Fourier transform of the propagator in Eq. (3). Integration of $G(\mathbf{q}, \omega)$ over the entire frequency domain yields

$$\int_{-\infty}^{\infty} G(\mathbf{q}, \omega) \frac{d\omega}{2\pi} = \langle S_{\mathbf{q}}^+ S_{-\mathbf{q}}^- \rangle. \quad (5)$$

The first moment of the frequency is given by

$$\begin{aligned} \langle \omega_{\mathbf{q}} \rangle &= \int_{-\infty}^{\infty} \omega G(\mathbf{q}, \omega) \frac{d\omega}{2\pi} \bigg/ \int_{-\infty}^{\infty} G(\mathbf{q}, \omega) \frac{d\omega}{2\pi} \\ &= \langle [S_{\mathbf{q}}^+, H_0] S_{-\mathbf{q}}^- \rangle / \langle S_{\mathbf{q}}^+ S_{-\mathbf{q}}^- \rangle. \end{aligned} \quad (6)$$

The commutator in the above equation has the explicit expression

$$[S_{\mathbf{q}}^+, H_0] = \frac{-J}{\sqrt{N}} \sum_{i, \delta} (S_i^z S_{i+\delta}^+ - S_i^+ S_{i+\delta}^z) e^{-i\mathbf{q} \cdot \mathbf{r}_i}. \quad (7)$$

Thus, the calculation of the first moment is reduced to the evaluation of two three-spin correlation functions and one two-spin correlation function. Similarly, the second moment can be written down in two different but equivalent expressions:

$$\begin{aligned} \langle \omega_{\mathbf{q}}^2 \rangle &= \langle [[S_{\mathbf{q}}^+, H_0], H_0] S_{-\mathbf{q}}^- \rangle / \langle S_{\mathbf{q}}^+ S_{-\mathbf{q}}^- \rangle \\ &= \langle [S_{\mathbf{q}}^+, H_0] [H_0, S_{-\mathbf{q}}^-] \rangle / \langle S_{\mathbf{q}}^+ S_{-\mathbf{q}}^- \rangle. \end{aligned} \quad (8)$$

The commutator $[H_0, S_{-\mathbf{q}}^-]$ has an expression similar to that in Eq. (7). The second moment, then, involves a few four-spin correlation functions. In this manner all higher moments of the frequency are expressed in terms of higher-order spin-correlation functions.

The evaluation of the spin-correlation functions requires approximations for the dynamical properties of the spins. At low temperatures one can employ the well-established Holstein-Primakoff transformation:⁸

$$\begin{aligned} S_i^z &= S - a_i^\dagger a_i, \\ S_i^- &= (2S)^{1/2} a_i^\dagger, \\ S_i^+ &= (2S)^{1/2} a_i, \end{aligned} \quad (9)$$

where a_i^\dagger and a_i are boson operators. Their Fourier transforms $a_{\mathbf{q}}^\dagger$ and $a_{\mathbf{q}}$ are the spin-wave or magnon operators. The evaluation of the first moment is entirely straightforward in the noninteracting spin-wave approximation, with the result

$$\begin{aligned} \langle \omega_{\mathbf{q}} \rangle &= 2zS \{1 - \gamma(\mathbf{q})\} - \frac{2z}{N} \sum_{\mathbf{q}_1} n(\mathbf{q}_1) \{1 - \gamma(\mathbf{q}) - \gamma(\mathbf{q}_1) \\ &\quad + \gamma(\mathbf{q} - \mathbf{q}_1)\}, \end{aligned} \quad (10)$$

where z is the number of nearest neighbors,

$$\gamma(\mathbf{q}) = \frac{1}{z} \sum_{\delta} e^{i\mathbf{q} \cdot \mathbf{r}_\delta}, \quad (11)$$

and \mathbf{r}_δ is the vector pointing from the site i to its nearest neighbor $i + \delta$. The first term in Eq. (10) can be recognized as the spin-wave energy in the linear spin-wave theory. In the

second term the quantity $n(\mathbf{q}) = \langle a_{\mathbf{q}}^\dagger a_{\mathbf{q}} \rangle$ is the occupation of the spin-wave state with wave vector \mathbf{q} . One can recognize the term as the Dyson correction to the spin-wave energy,⁹ which depends on the temperature T according to $T^{5/2}$.

The evaluation of the second moment requires some work. We will merely present the answer here because the algebra is straightforward. We can write

$$\langle \omega_{\mathbf{q}}^2 \rangle = \langle \omega_{\mathbf{q}} \rangle^2 + \langle \delta\omega_{\mathbf{q}}^2 \rangle, \quad (12)$$

where

$$\begin{aligned} \langle \delta\omega_{\mathbf{q}}^2 \rangle &= \frac{2z^2}{N^2} \sum_{\mathbf{q}_1, \mathbf{q}_2} \frac{n(\mathbf{q}_1 + \mathbf{q}_2 - \mathbf{q}) [1 + n(\mathbf{q}_1)] [1 + n(\mathbf{q}_2)]}{1 + n(\mathbf{q})} \\ &\quad \times \{ \gamma(\mathbf{q}_1) + \gamma(\mathbf{q}_2) - \gamma(\mathbf{q} - \mathbf{q}_1) - \gamma(\mathbf{q} - \mathbf{q}_2) \}^2. \end{aligned} \quad (13)$$

As long as $\langle \omega_{\mathbf{q}} \rangle \gg \{ \langle \delta\omega_{\mathbf{q}}^2 \rangle \}^{1/2}$, the former is the position and the latter is the width of the spin-wave peak, both are directly measurable by neutron scattering experiments. The linewidth result in Eq. (13) can be calculated from the scattering of two spin waves as formulated by Dyson.⁹ Thus, the moment method is capable of reproducing the results of a highly sophisticated theory using the lowest-order boson approximation for the spin operators.

III. THE SINUSOIDALLY MODULATED SPIN STRUCTURE

In this section we give a brief review of the Nishikubo-Nagamiya³ theory of the stability of the sinusoidal spin structure, with the added detail that both Er and Tm has the hexagonal-closed-packed (hcp) crystal structure, with two inequivalent sites per unit cell. We label the two sublattices by the index $l=1,2$, the position vectors of the two lattice sites by \mathbf{r}_i and $\mathbf{r}_i + \boldsymbol{\tau}$, and the spins on the sublattices by \mathbf{S}_{li} . The spin Hamiltonian is

$$H = - \sum_{ij} J_{ij} \mathbf{S}_{li} \cdot \mathbf{S}_{lj} - \sum_{ij} J'_{ij} \mathbf{S}_{li} \cdot \mathbf{S}_{l',j} - K \sum_i (S_{li}^z)^2, \quad (14)$$

where $l' = l + 1 \pmod{2}$, the indices i, j sum over all unit cells, J_{ij} denotes the long-range exchange coupling between two spins on sites in the same sublattice, J'_{ij} the exchange coupling between two sites in opposite sublattices, and K is the single-site twofold anisotropy constant.

The mean field at site i of the sublattice 1 is

$$H_{1i}^z = 2 \sum_j J_{ij} S_{1j}^z + 2 \sum_j J'_{ij} S_{2j}^z + 2K S_{1i}^z. \quad (15)$$

An interchange of the sublattice indices 1 and 2 yields the expression for the mean field at a site i of the sublattice 2. For a sinusoidal moment distribution with \mathbf{q} along the c axis, we write the ordered part of the moments as

$$\langle S_{1i}^z \rangle = m \cos\{\mathbf{q} \cdot \mathbf{r}_i\},$$

and

$$\langle S_{2i}^z \rangle = m \cos\{\mathbf{q} \cdot (\mathbf{r}_i + \boldsymbol{\tau})\}. \quad (16)$$

Putting these expressions into Eq. (15), we obtain

$$H_{ii}^z = 2\langle S_{ii}^z \rangle \{ \mathcal{J}(\mathbf{q}) + \mathcal{J}'(\mathbf{q}) + K \}, \quad (17)$$

where

$$\mathcal{J}(\mathbf{q}) = \sum_j J_{ij} e^{i\mathbf{q} \cdot \mathbf{r}_{ij}},$$

$\mathbf{r}_{ij} = \mathbf{r}_i - \mathbf{r}_j$, and

$$\mathcal{J}'(\mathbf{q}) = \sum_j J'_{ij} e^{i\mathbf{q} \cdot (\mathbf{r}_{ij} + \boldsymbol{\tau})}. \quad (18)$$

The mean-field equation is

$$\langle S_{ii}^z \rangle = S B_S(\beta H_{ii}^z), \quad (19)$$

where $\beta = 1/k_B T$, T is the temperature, and B_S is the Brillouin function. This equation yields a nonzero solution for the ordered moment for $T < T_N$, where the Néel temperature T_N satisfies

$$k_B T_N = \frac{2}{3} S(S+1) \{ \mathcal{J}_T(\mathbf{Q}) + K \}, \quad (20)$$

where $\mathcal{J}_T(\mathbf{Q}) = \mathcal{J}(\mathbf{Q}) + \mathcal{J}'(\mathbf{Q})$. In Eq. (20) the vector \mathbf{Q} maximizes the total exchange energy $\mathcal{J}_T(\mathbf{q})$ for all vectors \mathbf{q} . Just below the Néel temperature the ordered moment has the temperature dependence $m \propto (T_N - T)^{1/2}$. The nonlinear nature of the mean-field theory in Eq. (19) predicts that at temperatures sufficiently below T_N the ordered moments develop higher harmonics such that the moment distribution tends to square up, as shown by McEwen *et al.*¹⁰

The helical spin state, for which the spins are all perpendicular to the c axis, can compete energetically with the sinusoidal state. The energy of the system in the sinusoidal state is

$$E = -N [\mathcal{J}_T(\mathbf{Q}) + K] m^2, \quad (21)$$

where N is the number of lattice sites, $N/2$ on each sublattice. In the helical state, however, the exchange energy is twice as large but the anisotropy energy is absent, i.e.,

$$E' = -2N [\mathcal{J}_T(\mathbf{Q})] m^2. \quad (22)$$

We ignore the difference in the magnetizations of the two states. It then follows that the sinusoidal state is stable provided that

$$K > \mathcal{J}_T(\mathbf{Q}). \quad (23)$$

This puts some constraint on the range of the energy parameters we may choose to fit the experimental results.

In the next section we will formulate the frequency moment calculation in terms of many-spin correlation functions, which in turn, are evaluated under a suitable approximation scheme. The scheme we choose involves two basic rules: (1) the ordered moment is factored out as a constant of motion, and (2) multiple spin-correlation functions are factored into products of two-spin correlation functions. The first rule is appropriate for condensed systems, and the second rule assumes that spin excitations are noninteracting modes, even at elevated temperatures where the sinusoidal structure exists. As we have learned from the ferromagnetic problem, one can use a primitive approximation and obtain a highly sophisti-

cated result. We believe the same principle also holds in the sinusoidal phase so that the results of our calculation are sufficiently accurate to guide the interpretation of experimental findings.

The two-spin correlation functions are calculated by relating them to staggered field susceptibilities.¹¹ For the longitudinal correlation function, we add a staggered field to the spins in sublattice 1 so that H_{1i}^z now has the form

$$H_{1i}^z = 2 \sum_j J_{ij} S_{1j}^z + 2 \sum_j J'_{ij} S_{2j}^z + 2K S_{1i}^z + h e^{i\mathbf{q} \cdot \mathbf{r}_{1i}}, \quad (24)$$

where \mathbf{q} is the wave vector of the staggered field. The mean field on sublattice 2 does not have the added term. We define the longitudinal susceptibilities $\chi_{ii}^{zz}(\mathbf{q})$ by

$$\langle S_{ii}^z \rangle = \chi_{ii}^{zz}(\mathbf{q}) h e^{i\mathbf{q} \cdot \mathbf{r}_{1i}}. \quad (25)$$

The linearized mean-field equation, which applies when $T > T_N$, yields the following equations for the susceptibilities:

$$\frac{3k_B T}{S(S+1)} \chi_{11}^{zz}(\mathbf{q}) = 2 \{ \mathcal{J}(\mathbf{q}) + K \} \chi_{11}^{zz}(\mathbf{q}) + 2 \mathcal{J}'(\mathbf{q}) \chi_{21}^{zz}(\mathbf{q}) + 1,$$

$$\frac{3k_B T}{S(S+1)} \chi_{21}^{zz}(\mathbf{q}) = 2 \{ \mathcal{J}(\mathbf{q}) + K \} \chi_{21}^{zz}(\mathbf{q}) + 2 \mathcal{J}'^*(\mathbf{q}) \chi_{11}^{zz}(\mathbf{q}). \quad (26)$$

In the above equations the quantities $\mathcal{J}(\mathbf{q})$ and $\mathcal{J}'(\mathbf{q})$ have been defined in Eq. (18). Notice that $\mathcal{J}(\mathbf{q})$ is real because the sublattices have inversion symmetry, whereas $\mathcal{J}'(\mathbf{q})$ is complex for general \mathbf{q} except when \mathbf{q} is parallel to the c axis. The solutions of these equations are

$$\chi_{11}^{zz}(\mathbf{q}) = \{ 3k_B T / S(S+1) - 2 \mathcal{J}(\mathbf{q}) - 2K \} / D,$$

and

$$\chi_{21}^{zz}(\mathbf{q}) = 2 \mathcal{J}'^*(\mathbf{q}) / D, \quad (27)$$

where

$$D = \{ 3k_B T / S(S+1) - 2 \mathcal{J}(\mathbf{q}) - 2K \}^2 + 4 | \mathcal{J}'(\mathbf{q}) |^2. \quad (28)$$

In a similar manner, we apply a staggered field on spins in sublattice 2 and find that $\chi_{22}^{zz}(\mathbf{q}) = \chi_{11}^{zz}(\mathbf{q})$ and $\chi_{12}^{zz}(\mathbf{q}) = [\chi_{21}^{zz}(\mathbf{q})]^*$. At $T = T_N$ we make use of the equation for T_N , Eq. (20), to write

$$\chi_{11}^{zz}(\mathbf{q}) = \chi_{22}^{zz}(\mathbf{q}) = 2 \{ \mathcal{J}_T(\mathbf{Q}) - \mathcal{J}(\mathbf{q}) \} / D, \quad (29)$$

where

$$D = 4 \{ [\mathcal{J}_T(\mathbf{Q}) - \mathcal{J}(\mathbf{q})]^2 - | \mathcal{J}'(\mathbf{q}) |^2 \}. \quad (30)$$

The expressions for the off-diagonal elements of χ remain the same except that the new expression for D are used. For $T < T_N$ we approximate the susceptibility matrix elements by their values at T_N . A better calculation can be carried out, but the expressions are much more complicated so that the essential physics becomes quite obscure.¹¹⁻¹³

We finally relate the susceptibilities to the correlation functions¹¹

$$\langle S_{1\mathbf{q}}^z S_{1-\mathbf{q}}^z \rangle = \langle S_{2\mathbf{q}}^z S_{2-\mathbf{q}}^z \rangle \equiv L_1(\mathbf{q}) = k_B T \chi_{11}^{zz}(\mathbf{q}), \quad (31)$$

$$\langle S_{2\mathbf{q}}^z S_{1,-\mathbf{q}}^z \rangle^* = \langle S_{1\mathbf{q}}^z S_{2,-\mathbf{q}}^z \rangle \equiv L_2(\mathbf{q}) = k_B T \chi_{12}^{zz}(\mathbf{q}).$$

In the above equations the Fourier transforms of the spins are defined in analogy with Eq. (2), i.e.,

$$\mathbf{S}_{l\mathbf{q}} = \sqrt{\frac{2}{N}} \sum_i \mathbf{S}_{li} e^{i\mathbf{q} \cdot \mathbf{r}_{li}}, \quad (32)$$

where $\mathbf{r}_{li} = \mathbf{r}$ for $l=1$ and $\mathbf{r} + \boldsymbol{\tau}$ for $l=2$. The longitudinal correlation functions diverge as $\mathbf{q} \rightarrow \mathbf{Q}$, as a necessary consequence of the long-range sinusoidal spin order.

For the transverse susceptibilities and two-spin correlation functions, we apply a staggered field perpendicular to the ordered moments. For instance, a staggered field in the x direction on the spins of sublattice 1 gives rise to the following mean field on sublattice 1:

$$H_{1i}^x = 2 \sum_j J_{ij} S_{1j}^x + 2 \sum_j J'_{ij} S_{2j}^x + h e^{i\mathbf{q} \cdot \mathbf{r}_{1i}}. \quad (33)$$

It differs from the mean field in Eq. (21) in that the anisotropy term does not contribute. An identical calculation yields the following transverse susceptibilities:

$$\chi_{11}^{xx}(\mathbf{q}) = \{3k_B T / S(S+1) - 2 \mathcal{F}(\mathbf{q})\} / D',$$

and

$$\chi_{21}^{xx}(\mathbf{q}) = 2 \mathcal{F}'^*(\mathbf{q}) / D', \quad (34)$$

where

$$D' = \{3k_B T / S(S+1) - 2 \mathcal{F}(\mathbf{q})\}^2 + 4 |\mathcal{F}'(\mathbf{q})|^2. \quad (35)$$

Below T_N we approximate the susceptibilities by their values at T_N , i.e.,

$$\chi_{11}^{xx}(\mathbf{q}) = 2 \{ \mathcal{F}_T(\mathbf{Q}) - \mathcal{F}(\mathbf{q}) + K \} / D',$$

where

$$D' = 4 \{ \mathcal{F}_T(\mathbf{q}) - \mathcal{F}(\mathbf{q}) + K \}^2 + 4 |\mathcal{F}'(\mathbf{q})|^2. \quad (36)$$

Finally

$$\begin{aligned} \langle S_{1\mathbf{q}}^x S_{1,-\mathbf{q}}^x \rangle &= \langle S_{2\mathbf{q}}^x S_{2,-\mathbf{q}}^x \rangle \equiv T_1(\mathbf{q}) = k_B T \chi_{11}^{xx}(\mathbf{q}), \\ \langle S_{2\mathbf{q}}^x S_{1,-\mathbf{q}}^x \rangle^* &= \langle S_{1\mathbf{q}}^x S_{2,-\mathbf{q}}^x \rangle \equiv T_2(\mathbf{q}) = k_B T \chi_{12}^{xx}(\mathbf{q}). \end{aligned} \quad (37)$$

There is complete symmetry between the two transverse directions x and y , so the two-spin correlation functions in the y directions are also given by the above equations.

IV. TRANSVERSE EXCITATIONS IN THE SINUSOIDAL PHASE

The spectral density for the transverse excitations is defined as the Fourier transform of the Green's function:

$$G(\mathbf{q}, t) = \langle T S_{\mathbf{q}}^x(t) S_{-\mathbf{q}}^x(0) \rangle. \quad (38)$$

The moments of the frequency are calculated in analogy with Eq. (6). For instance,

$$\langle \omega_{\mathbf{q}} \rangle = \langle [S_{\mathbf{q}}^x, H] S_{-\mathbf{q}}^x \rangle / \langle S_{\mathbf{q}}^x S_{-\mathbf{q}}^x \rangle, \quad (39)$$

where H is the Hamiltonian in Eq. (14), and

$$\mathbf{S}_{\mathbf{q}} = N^{1/2} \sum_{l=1}^2 \sum_i \mathbf{S}_{li} e^{i\mathbf{q} \cdot \mathbf{r}_{li}} = 2^{-1/2} (\mathbf{S}_{1\mathbf{q}} + \mathbf{S}_{2\mathbf{q}}).$$

The Fourier components $\mathbf{S}_{l\mathbf{q}}$ have been defined in Eq. (32). The commutator $[S_{l\mathbf{q}}^x, H]$ can be evaluated readily:

$$\begin{aligned} [S_{1\mathbf{q}}^x, H] &= i \left(\frac{2}{N} \right)^{1/2} \sum_{\mathbf{q}_1} 2 \{ [K - \mathcal{F}(\mathbf{q} - \mathbf{q}_1) \\ &\quad + \mathcal{F}(\mathbf{q}_1)] S_{1\mathbf{q}_1}^z S_{1,\mathbf{q}-\mathbf{q}_1}^y + \mathcal{F}'^*(\mathbf{q}_1) S_{2\mathbf{q}_1}^z S_{1,\mathbf{q}-\mathbf{q}_1}^y \\ &\quad - \mathcal{F}'^*(\mathbf{q} - \mathbf{q}_1) S_{1\mathbf{q}_1}^z S_{2,\mathbf{q}-\mathbf{q}_1}^y \}. \end{aligned} \quad (40)$$

The expression for $[S_{2\mathbf{q}}^x, H]$ is similar. According to the approximation scheme in the last section, we decouple the ordered moment by factoring out

$$S_{l\mathbf{q}_1}^z = \frac{m}{2} \left(\frac{N}{2} \right)^{1/2} [\delta_{\mathbf{q}_1, \mathbf{Q}} + \delta_{\mathbf{q}_1, -\mathbf{Q}}]. \quad (41)$$

The result after this step is

$$\begin{aligned} [S_{1\mathbf{q}}^x, H] &= im \{ [K - \mathcal{F}_T(\mathbf{q} - \mathbf{Q}) + \mathcal{F}_T(\mathbf{Q})] S_{1,\mathbf{q}-\mathbf{Q}}^y \\ &\quad + (\mathbf{Q} \rightarrow -\mathbf{Q}) \}, \end{aligned} \quad (42)$$

and a similar result for $[S_{2\mathbf{q}}^x, H]$. What is left in the numerator of Eq. (39) is a correlation function between S^y and S^x , which is zero according to the results of the last section. Therefore, the first moment of the frequency vanishes. In a similar way, we find that all odd moments of the frequency vanish. The spectral function $G(\mathbf{q}, \omega)$ is an even function of the frequency ω .

We assume a simple and practical form of $G(\mathbf{q}, \omega)$ as follows:

$$G(\mathbf{q}, \omega) = C [e^{-(\omega + \Omega_{\mathbf{q}})^2 / 2\Gamma_{\mathbf{q}}^2} + e^{-(\omega - \Omega_{\mathbf{q}})^2 / 2\Gamma_{\mathbf{q}}^2}], \quad (43)$$

where C is a normalization constant, and $\Omega_{\mathbf{q}}$ and $\Gamma_{\mathbf{q}}$ are two fitting parameters. The spectrum has either two resolved peaks or one broad peak depending on whether the ratio $\Omega_{\mathbf{q}} / \Gamma_{\mathbf{q}}$ is greater or less than unity. It follows that

$$\langle \omega_{\mathbf{q}}^2 \rangle = \Omega_{\mathbf{q}}^2 + \Gamma_{\mathbf{q}}^2 \quad (44a)$$

and

$$\langle \omega_{\mathbf{q}}^4 \rangle = \Omega_{\mathbf{q}}^4 + 6\Omega_{\mathbf{q}}^2 \Gamma_{\mathbf{q}}^2 + 3\Gamma_{\mathbf{q}}^4. \quad (44b)$$

The two fitting parameters, and therefore the line shape, are determined by the second and fourth moments of the frequency.

As in the ferromagnetic problem, the second moment can be calculated in two ways. The first method requires the calculation of a double commutator:

$$\langle \omega_{\mathbf{q}}^2 \rangle = \langle [[S_{\mathbf{q}}^x, H], H] S_{-\mathbf{q}}^x \rangle / \langle S_{\mathbf{q}}^x S_{-\mathbf{q}}^x \rangle. \quad (45)$$

The calculation is greatly simplified when the ordered moment is decoupled along the way. The final answer is quite lengthy to write down except in the experimentally practical case where $\mathbf{q} \parallel \mathbf{Q}$:

$$\langle \omega_{\mathbf{q}}^2 \rangle = m^2 [K + \mathcal{F}_T(\mathbf{Q}) - \mathcal{F}_T(\mathbf{q})] [2K + 2\mathcal{F}_T(\mathbf{Q}) - \mathcal{F}_T(\mathbf{q} + \mathbf{Q}) - \mathcal{F}_T(\mathbf{q} - \mathbf{Q})], \quad (46)$$

where $\mathcal{F}_T(\mathbf{q}) = \mathcal{F}(\mathbf{q}) + \mathcal{F}'(\mathbf{q})$, as defined under Eq. (20), is real. The second method involves two single commutators:

$$\langle \omega_{\mathbf{q}}^2 \rangle = \langle [S_{\mathbf{q}}^x, H][H, S_{-\mathbf{q}}^x] \rangle / \langle S_{\mathbf{q}}^x S_{-\mathbf{q}}^x \rangle. \quad (47)$$

Although the two methods are equivalent, we need to check whether they yield the same answer under the approximation scheme developed in the last section. Direct calculation gives, again for $\mathbf{q} \parallel \mathbf{Q}$, the result

$$\langle \omega_{\mathbf{q}}^2 \rangle = m^2 \{ [K - \mathcal{F}_T(\mathbf{q} - \mathbf{Q}) + \mathcal{F}_T(\mathbf{Q})]^2 T(\mathbf{q} - \mathbf{Q}) + [K - \mathcal{F}_T(\mathbf{q} + \mathbf{Q}) + \mathcal{F}_T(\mathbf{Q})]^2 T(\mathbf{q} + \mathbf{Q}) \} / T(\mathbf{q}), \quad (48)$$

where

$$\begin{aligned} T(\mathbf{q}) &= T_1(\mathbf{q}) + T_2(\mathbf{q}) \\ &= k_B T / 2 [K + \mathcal{F}_T(\mathbf{Q}) - \mathcal{F}_T(\mathbf{q})] \end{aligned} \quad (49)$$

is real when \mathbf{q} is parallel to the c axis. Substituting Eq. (49) into Eq. (48), we verify that the new result is the same as that in Eq. (46). Thus, the approximation scheme we have developed is internally consistent.

It is instructive to contrast the result for $\langle \omega_{\mathbf{q}}^2 \rangle$ in Eq. (46) with the spin-wave dispersion relation in the helical phase:^{14,15}

$$\begin{aligned} \omega_{\mathbf{q}}^2 &= 2m^2 [K + \mathcal{F}_T(\mathbf{Q}) - \mathcal{F}_T(\mathbf{q})] \\ &\times [2\mathcal{F}_T(\mathbf{Q}) - \mathcal{F}_T(\mathbf{q} + \mathbf{Q}) - \mathcal{F}_T(\mathbf{q} - \mathbf{Q})]. \end{aligned}$$

With moments in the basal plane, the anisotropy energy K appears at different places. Concentrating on the exchange energy contribution, we find that the right-hand side of the above expression is twice the result in Eq. (46). Recall that in the helical phase all spins have the same expectation value m whereas in the sinusoidal phase the moments vary sinusoidally, one can see that the factor of one-half for the sinusoidal phase comes from averaging the square of the moments. This local variation in moments gives rise to a local fluctuation in exchange energy and consequently a broadening of the spin-wave energy.

The calculation of the fourth moment proceeds as follows. We start from the formula

$$\langle \omega_{\mathbf{q}}^4 \rangle = \langle [[S_{\mathbf{q}}^x, H], H][H, [H, S_{-\mathbf{q}}^x]] \rangle / \langle S_{\mathbf{q}}^x S_{-\mathbf{q}}^x \rangle, \quad (50)$$

evaluate the commutators according to Eq. (40) while simplify the interim result by decoupling the ordered moment. For general \mathbf{q} the final formula for the fourth moment is quite complex, but in the restricted case when \mathbf{q} is in the c -axis direction the formula simplifies. We obtain

$$\langle \omega_{\mathbf{q}}^4 \rangle - (\langle \omega_{\mathbf{q}}^2 \rangle)^2 = \langle (\delta \omega_{\mathbf{q}}^2)^2 \rangle,$$

where

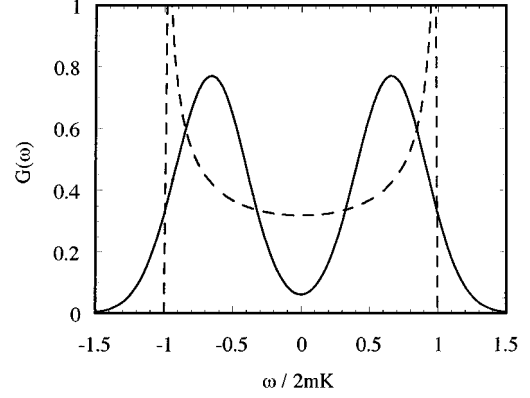


FIG. 1. The frequency spectrum of transverse magnetic excitations in a sinusoidal spin system for which the twofold anisotropy energy is much stronger than the exchange energy. The dotted curve is the exact spectrum, and the solid curve is the double Gaussian approximation which has the same second and fourth moments as the exact spectrum.

$$\begin{aligned} \langle (\delta \omega_{\mathbf{q}}^2)^2 \rangle &= m^4 [K - \mathcal{F}_T(\mathbf{q}) + \mathcal{F}_T(\mathbf{Q})] \{ [K - \mathcal{F}_T(\mathbf{q} - \mathbf{Q}) \\ &+ \mathcal{F}_T(\mathbf{Q})]^2 [K - \mathcal{F}_T(\mathbf{q} - 2\mathbf{q}) + \mathcal{F}_T(\mathbf{Q})]^2 \\ &\times T(\mathbf{q} - 2\mathbf{Q}) + (\mathbf{Q} \rightarrow -\mathbf{Q}) \} / T(\mathbf{q}). \end{aligned} \quad (51)$$

In the limit of strong twofold anisotropy, the frequency spectrum has a simple analytical form:⁵

$$G(\omega) = \frac{1}{\pi} (4m^2 K^2 - \omega^2)^{-1/2}, \quad (52)$$

for $|\omega| < 2mK$ and zero otherwise. This result follows because the frequency spectrum reflects the distribution of the local anisotropy gap given by

$$\omega_{li} = 2mK \cos(\mathbf{Q} \cdot \mathbf{r}_{li}). \quad (53)$$

The frequency spectrum is dispersionless. It is straightforward to calculate the second and fourth moments, with the results $\langle \omega^2 \rangle = 2m^2 K^2$ and $\langle \omega^4 \rangle = 6m^4 K^4$. These are in complete agreement with the limiting values of Eqs. (46) and (51). The comparison between the exact spectrum and the fitted spectrum in Eq. (43) is shown in Fig. 1. The two spectra agree in that they both exhibit the two peak structure. It is not possible to reproduce the singularities of the exact spectrum in Eq. (52) by the double Gaussian form in Eq. (43).

The observed spin excitation spectrum in the sinusoidal phase of Tm agrees with our high anisotropy result in Eq. (52).^{10,16} The spectrum for Er is explained by the opposite condition, that the exchange energy is strong compared with the anisotropy energy.⁵ This will be discussed further in Sec. VI.

V. LONGITUDINAL EXCITATIONS IN THE SINUSOIDAL PHASE

As in the transverse case, the odd moments of the frequency vanish for the longitudinal excitations. The second and fourth moments of the frequency are calculated from evaluating the following spin-correlation functions:

$$\langle \omega_{\mathbf{q}}^2 \rangle = \langle [S_{\mathbf{q}}^z, H][H, S_{-\mathbf{q}}^z] \rangle / \langle S_{\mathbf{q}}^z S_{-\mathbf{q}}^z \rangle, \quad (54)$$

and

$$\langle \omega_{\mathbf{q}}^4 \rangle = \langle [[S_{\mathbf{q}}^z, H], H][H, [H, S_{-\mathbf{q}}^z]] \rangle / \langle S_{\mathbf{q}}^z S_{-\mathbf{q}}^z \rangle. \quad (55)$$

The commutator $[S_{\mathbf{q}}^z, H]$ can be readily evaluated:

$$\begin{aligned} [S_{\mathbf{q}}^z, H] &= i \left(\frac{2}{N} \right)^{1/2} \sum_{\mathbf{q}_1} 2 \{ [\mathcal{F}(\mathbf{q}-\mathbf{q}_1) - \mathcal{F}(\mathbf{q}_1)] S_{\mathbf{q}_1}^x S_{\mathbf{q}-\mathbf{q}_1}^y \\ &\quad + \mathcal{F}'(\mathbf{q}-\mathbf{q}_1) S_{\mathbf{q}_1}^x S_{2, \mathbf{q}-\mathbf{q}_1}^y - \mathcal{F}'(\mathbf{q}_1) S_{2\mathbf{q}_1}^x S_{1, \mathbf{q}-\mathbf{q}_1}^y \}. \end{aligned} \quad (56)$$

The expression for $[S_{2\mathbf{q}}^z, H]$ is similar. The operator $S_{\mathbf{q}}^z$ does not appear in the above result, so we cannot factor out the ordered moment in this step. In the numerator of the second moment expression we encounter four-spin correlation functions of the form

$$\begin{aligned} \langle S_{l_1, \mathbf{q}_1}^x S_{l_2, \mathbf{q}_2}^y S_{l_3, \mathbf{q}_3}^x S_{l_4, \mathbf{q}_4}^y \rangle \\ \simeq \delta_{\mathbf{q}_1, -\mathbf{q}_4} \delta_{\mathbf{q}_2, -\mathbf{q}_3} \langle S_{l_1, \mathbf{q}_1}^x S_{l_1, -\mathbf{q}_1}^x \rangle \langle S_{l_2, \mathbf{q}_2}^y S_{l_2, -\mathbf{q}_2}^y \rangle, \end{aligned}$$

by applying the rules of approximation developed in Sec. III. Depending on the sublattice label, the two-spin correlation functions are to be identified with $T_1(\mathbf{q}_n)$ or $T_2(\mathbf{q}_n)$, respectively. After considerable algebraic manipulations, we find the final formula for the second moment:

$$\begin{aligned} \langle \omega_{\mathbf{q}}^2 \rangle &= \frac{16}{N} [\mathcal{F}_T(\mathbf{Q}) - \mathcal{F}_T(\mathbf{q})] \\ &\quad \times \sum_{\mathbf{q}_1} \{ [\mathcal{F}(\mathbf{q}-\mathbf{q}_1) - \mathcal{F}(\mathbf{q})] T_1(\mathbf{q}-\mathbf{q}_1) \\ &\quad - \text{Re}[\mathcal{F}'(\mathbf{q}-\mathbf{q}_1) - \mathcal{F}'^*(\mathbf{q}_1)] T_2(\mathbf{q}-\mathbf{q}_1) \}. \end{aligned} \quad (57)$$

We have also verified that the formula $\langle \omega_{\mathbf{q}}^2 \rangle = \langle [[S_{\mathbf{q}}^z, H], H] S_{-\mathbf{q}}^z \rangle / \langle S_{\mathbf{q}}^z S_{-\mathbf{q}}^z \rangle$ yields the same result for the second moment as given in Eq. (57). Notice that we can not simplify the expression by restricting $\mathbf{q} \parallel \mathbf{Q}$ because the sum over \mathbf{q}_1 extends over the entire Brillouin zone.

The evaluation of the fourth moment requires a great deal of work. We again write

$$\langle \omega_{\mathbf{q}}^4 \rangle = \langle (\omega_{\mathbf{q}}^2)^2 \rangle + \langle (\delta \omega_{\mathbf{q}}^2)^2 \rangle, \quad (58)$$

where

$$\begin{aligned} \langle (\delta \omega_{\mathbf{q}}^2)^2 \rangle &= \frac{m^2}{2k_B T} [\mathcal{F}_T(\mathbf{Q}) - \mathcal{F}_T(\mathbf{q})] \frac{1}{N} \\ &\quad \times \sum_{\mathbf{q}_1} [A(\mathbf{q}_1, \mathbf{q}, \mathbf{Q}) + A(\mathbf{q}_1, \mathbf{q}, -\mathbf{Q})], \end{aligned} \quad (59)$$

and $A(\mathbf{q}_1, \mathbf{q}, \mathbf{Q})$ is a complicated expression involving the exchange and anisotropy parameters:

$$\begin{aligned} A(\mathbf{q}_1, \mathbf{q}, \mathbf{Q}) &= [|B_1|^2 + |B_2|^2] T_1(\mathbf{q}_1 - \mathbf{Q}) T_1(\mathbf{q} - \mathbf{q}_1) \\ &\quad + 4 T_1(\mathbf{q}_1 - \mathbf{Q}) \text{Re}[B_1^* B_2 T_2(\mathbf{q} - \mathbf{q}_1)] \\ &\quad + \text{Re}[B_1^2 T_2^*(\mathbf{q}_1 - \mathbf{Q}) T_2^*(\mathbf{q} - \mathbf{q}_1)] \\ &\quad + \frac{1}{2} \text{Re}[B_2^{*2} T_2(\mathbf{q}_1 - \mathbf{Q}) T_2^*(\mathbf{q} - \mathbf{q}_1)], \end{aligned} \quad (60)$$

$$B_1 = C_1(\mathbf{q}_1) + C_1(\mathbf{q} - \mathbf{q}_1 + \mathbf{Q}),$$

$$B_2 = C_2(\mathbf{q}_1) + C_2^*(\mathbf{q} - \mathbf{q}_1 + \mathbf{Q}), \quad (61)$$

$$\begin{aligned} C_1(\mathbf{q}_1) &= 4 \{ [\mathcal{F}(\mathbf{q}-\mathbf{q}_1) - \mathcal{F}(\mathbf{q}_1)] [\mathcal{F}_T(\mathbf{Q}) - \mathcal{F}_T(\mathbf{Q}-\mathbf{q}_1) + K] \\ &\quad - [\mathcal{F}'^*(\mathbf{q}-\mathbf{q}_1) - \mathcal{F}'(\mathbf{q}_1)] \mathcal{F}'^*(\mathbf{q}_1 - \mathbf{Q}) \}, \\ C_2(\mathbf{q}_1) &= 4 \{ [\mathcal{F}'^*(\mathbf{q}-\mathbf{q}_1) - \mathcal{F}'(\mathbf{q}_1)] \\ &\quad \times [\mathcal{F}_T(\mathbf{Q}) - \mathcal{F}_T(\mathbf{Q}-\mathbf{q}_1) + K] \\ &\quad - [\mathcal{F}(\mathbf{q}-\mathbf{q}_1) - \mathcal{F}(\mathbf{q}_1)] \mathcal{F}'(\mathbf{q}_1 - \mathbf{Q}) \}. \end{aligned} \quad (62)$$

We consider for the moment the analytical properties of the results in Eqs. (57) and (59). It is clearly seen that both the second and the fourth moments vanish when $\mathbf{q} = \pm \mathbf{Q}$, which means that there is an undamped zero-frequency mode at each magnetic satellite point. These are just the Goldstone modes which characterize the translational invariance of the sinusoidal moment structure. Away from the satellites we find damped modes with linear dispersion relation $\omega_{\mathbf{q}} \propto |\mathbf{q} - \mathbf{Q}|$. This conclusion is in qualitative agreement with the experiment on Er.⁶ For Tm whose anisotropy energy far exceeds the exchange energy, both the second and the fourth moments are small because they are of the order of $\mathcal{F}_T(\mathbf{Q})/K$. Our theory predicts that it will be difficult to observe the longitudinal mode except very near the magnetic satellite point. Further comparison with experimental data will be the subject of the next section.

VI. COMPARISON WITH EXPERIMENTAL RESULTS ON Er

We have shown that the determination of the magnetic excitation spectra requires the complete knowledge of the long-range interaction parameters J_{ij} and J'_{ij} as well as the anisotropy constant K in the sinusoidal phase of Er. In reality, what we know about these parameters are culled from low-temperature spin-wave measurements when Er is in the conical phase.¹⁷ In this structure all spins in the same hexagonal plane are aligned parallel to one another. The net moment of each layer points at an angle away from the c axis such that there is a net ferromagnetic moment parallel to the c axis. The basal plane component of the net moments form a helical structure. The anisotropy energies in this phase is expected to be very different from that in the sinusoidal phase. The exchange parameters are also different for these two spin structures because they have different c axis periodicities. Since only the spin-wave spectrum for \mathbf{q} in the c -axis direction has been measured, it is possible to determine at most the Fourier transform $\mathcal{F}_T(\mathbf{q})$ for \mathbf{q} in this direction. To compound the uncertainty, Nicklow *et al.* re-

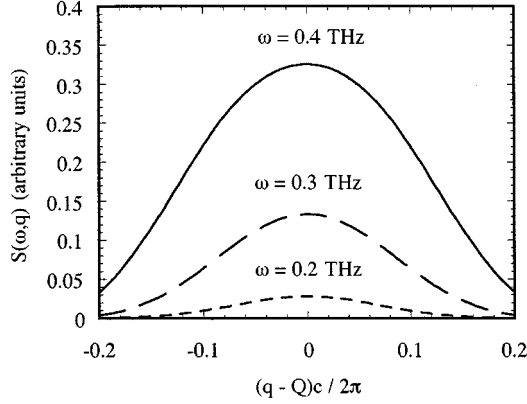


FIG. 2. Calculated constant energy scan neutron-scattering cross sections for transverse spin excitations at three different energies.

ported that it was not possible to fit their data by isotropic exchange and single-ion anisotropy terms alone.¹⁷ Different attempts to construct the model Hamiltonian yielded different sets of exchange parameters.^{17,18} Nevertheless, these empirical parameters are useful as a guide in our attempt to understand the experimental data for the sinusoidal phase.⁶

One can use the Néel temperature to obtain an estimate of the relevant energy scale of the magnetic excitations. Using Eq. (20) and the values $T_N=84$ K and $S=15/2$ to find $K + \mathcal{J}_T(\mathbf{Q})=0.165$ meV. Then the stability criterion for the sinusoidal phase, Eq. (23), implies that $0.165 > K > 0.083$ meV, and $0 < \mathcal{J}_T(\mathbf{Q}) < 0.083$ meV. These limits are applicable to the extent that the mean-field theory is accurate.

Near \mathbf{Q} where $\mathcal{J}_T(\mathbf{q})$ is maximum, we assume a parabolic shape

$$\mathcal{J}_T(\mathbf{q}) \approx \mathcal{J}_T(\mathbf{Q}) - a(\mathbf{q} - \mathbf{Q})^2, \quad (63)$$

where $a > 0$. We then factor out the energy scale $K + \mathcal{J}_T(\mathbf{Q})$ and write

$$\langle \omega_{\mathbf{q}}^2 \rangle = 2m^2 [K + \mathcal{J}_T(\mathbf{Q})] [K + a(\mathbf{q} - \mathbf{Q})^2] c_1(\mathbf{q}), \quad (64)$$

and

$$\langle (\delta \omega_{\mathbf{q}}^2)^2 \rangle = 2m^4 [K + \mathcal{J}_T(\mathbf{Q})]^3 [K + a(\mathbf{q} - \mathbf{Q})^2] c_2(\mathbf{q}), \quad (65)$$

where $c_1(\mathbf{q}), c_2(\mathbf{q})$ are dimensionless ratios of energy parameters, both of the order unity. We will ignore the \mathbf{q} dependence of c_1 and c_2 and treat them as fitting constants. We use the full moment $m = 15/2$ in order to compare the predictions of our theory with the experimental result in Ref. 6 taken at 60 K, which is about 70% of the Néel temperature. For the parameter a , we recall that Nicklow *et al.*¹⁷ and Lingård¹⁸ wrote

$$\mathcal{J}_T(\mathbf{q}) = \sum_{l=1}^n J_l \cos(lqc/2), \quad (66)$$

for \mathbf{q} in the c -axis direction. One can obtain estimates of a from the curvature of $\mathcal{J}_T(\mathbf{q})$ around its maximum. In this manner we find $a = 1.2$ meV/(2 πc)² from the fitting parameters in Ref. 17 and 1.8 meV/(2 πc)² from those in Ref. 18. We choose to use the latter value in our numerical analysis.

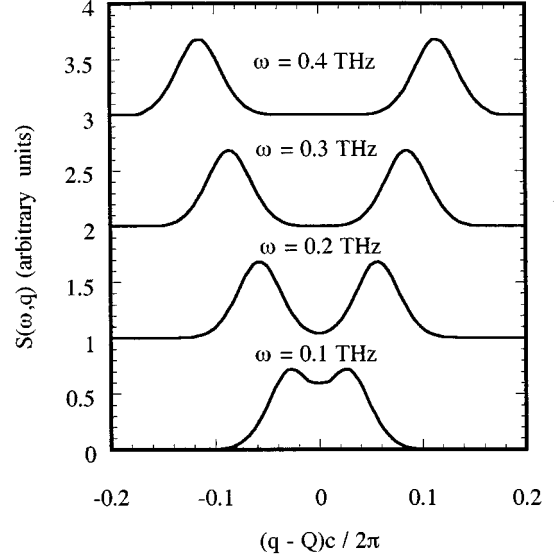


FIG. 3. Calculated constant energy scan neutron-scattering cross sections for longitudinal spin excitations at four different energies. The curves are shifted up from one another successively by one unit.

In Fig. 2 we show the calculated neutron-scattering cross section for three constant-energy scans as functions of the momentum transfer measured from \mathbf{Q} . The parameters are chosen so that the full width at half maximum of the line shape for $\omega = 0.3$ THz (1 THz \approx 4 meV) matches the published curve in Ref. 6. The fitting parameters are such that $K = 0.085$ meV, which is at the lower end of our estimated range, and $c_1 = 2.5$, $c_2 = 1.5$. Nicklow and Wakabayashi also reported that the transverse magnetic cross section becomes very weak at 0.5 THz and above.⁶ In our calculation, we find that the lines fade away at energies higher than 0.6 THz.

An accurate calculation of the frequency moments for the longitudinal mode is impossible because it requires the knowledge of $\mathcal{J}(\mathbf{q})$ and $\mathcal{J}'(\mathbf{q})$ over the entire Brillouin zone. We can, nevertheless, make progress by using a set of approximations similar to the transverse mode case. The quantity in the Brillouin zone sum involves exchange and anisotropy energies in both the numerator and the denominator. If we scale all quantities by the energy scale $K + \mathcal{J}_T(\mathbf{Q}) = 0.165$ meV, we can write

$$\langle \omega_{\mathbf{q}}^2 \rangle = 8k_B T_N [\mathcal{J}_T(\mathbf{Q}) - \mathcal{J}_T(\mathbf{q})] c_1'(\mathbf{q}), \quad (67)$$

and

$$\langle (\delta \omega_{\mathbf{q}}^2)^2 \rangle = m^2 k_B T_N [K + \mathcal{J}_T(\mathbf{Q})]^2 \times [\mathcal{J}_T(\mathbf{Q}) - \mathcal{J}_T(\mathbf{q})] c_2'(\mathbf{q}), \quad (68)$$

where $c_1'(\mathbf{q})$ and $c_2'(\mathbf{q})$ are dimensionless Brillouin zone sums. We ignore the \mathbf{q} dependence of the two sums and estimates them to be of the order unity. Together with the assumed form $\mathcal{J}_T(\mathbf{Q}) - \mathcal{J}_T(\mathbf{q}) = a(\mathbf{q} - \mathbf{Q})^2$, and the previously estimated value of a , we find that the measured peak positions and linewidths for the constant energy scan at 0.3

THz can be fitted by choosing $c'_1=1.7$ and $c'_2=1.1$. A set of the calculated line shapes for four different energies is shown in Fig. 3. The linear dispersion seen in the experiments is reproduced here. The calculated curves show that the linewidth increases only slightly with increasing energy transfer, and this is a direct consequence of our treating $c'_1(\mathbf{q})$ and $c'_2(\mathbf{q})$ as constants.

In summary, we have clarified the physics of the magnetic excitations in the sinusoidal spin phase of Er and Tm. The transverse excitations are broad lines centered around the reciprocal-lattice points, and the linewidth arises from the spatial variations of exchange and anisotropy energies, while the longitudinal excitations are extensions of the Goldstone

mode and are quite sharp. The velocity of the longitudinal mode is directly related to the spin-wave velocity at low temperatures.

ACKNOWLEDGMENTS

The authors are indebted to Dr. R. M. Nicklow and Dr. N. Wakabayashi for stimulating this investigation and for numerous helpful discussions. One of the authors (S.H.L.) would like to thank Professor R. C. Dynes and Professor L. J. Sham for their hospitality. This research was supported in part by the Division of Materials Sciences, U.S. Department of Energy under Contract No. W-7405-eng-26 with Martin Marietta Energy Systems, Inc.

-
- ¹W. C. Koehler, in *Magnetic Properties of Rare Earth Metals*, edited by R. J. Elliott (Plenum Press, London, 1972), Chap. 3.
- ²S. K. Sinha, in *Handbook on the Physics and Chemistry of Rare Earths*, edited by K. A. Gschneidner, Jr. and L. Eyring (North-Holland, Amsterdam, 1978), Vol. I, Chap. 5.
- ³T. Nishikubo and T. Nagamiya, *J. Phys. Soc. Jpn.* **20**, 808 (1965).
- ⁴B. R. Cooper, in *Solid State Physics*, edited by F. Seitz, D. Turnbull and H. Ehrenreich (Academic Press, New York, 1968), Vol. 21, p. 393.
- ⁵S. H. Liu, *J. Magn. Magn. Mater.* **22**, 93 (1980).
- ⁶R. M. Nicklow and N. Wakabayashi, *Phys. Rev. B* **26**, 3994 (1982).
- ⁷A. A. Maradudin, E. W. Montroll, G. H. Weiss, and I. P. Ipatova, *Solid State Physics*, 2nd ed. (Academic Press, New York, 1971), Suppl. 3, p. 174.
- ⁸T. Holstein and H. Primakoff, *Phys. Rev.* **58**, 1098 (1940).
- ⁹F. J. Dyson, *Phys. Rev.* **102**, 1217 (1956).
- ¹⁰K. A. KcEwen, U. Steigenberger, and J. Jensen, *Phys. Rev. B* **43**, 3298 (1990).
- ¹¹S. H. Liu, *Phys. Rev.* **139**, 1522 (1965).
- ¹²K. H. Lee and S. H. Liu, *Phys. Rev.* **159**, 390 (1967).
- ¹³H. Tanaka and K. Tani, *Prog. Theor. Phys.* **41**, 590 (1969).
- ¹⁴B. R. Cooper, R. J. Elliott, S. J. Nettel, and H. Suhl, *Phys. Rev.* **127**, 57 (1962).
- ¹⁵A. R. Mackintosh and H. Bjerrum Møller, *Magnetic Properties of Rare Earth Metals*, edited by R. J. Elliott (Plenum Press, London, 1972), Chap. 5.
- ¹⁶J. A. Fernandez-Baca, R. M. Nicklow, and J. J. Rhyne, *J. Appl. Phys.* **67**, 5283 (1990); J. A. Fernandez-Baca, R. M. Nicklow, Z. Tun, and J. J. Rhyne, *Phys. Rev. B* **43**, 3188 (1991).
- ¹⁷R. M. Nicklow, N. Wakabayashi, M. K. Wilkinson, and R. E. Reed, *Phys. Rev. Lett.* **27**, 334 (1971).
- ¹⁸P. A. Lingård, *Phys. Rev. B* **17**, 2348 (1978).